Supplementary Materials for

Visible-light-driven oxygen reduction by an anisotropically crystallized $CuBi_2O_4$ photocathode fabricated using a mixed metal-imidazole casting method

Ryohei Sekine, Tetsuya Sato, Zaki N. Zahran*, Yuta Tsubonouchi, Debraj Chandra, Norihisa Hoshino and Masayuki Yagi*.

Department of Materials Science and Technology, Faculty of Engineering, Niigata University, 8050 Ikarashi-2, Niigata 9050-2181, Japan.

*Correspondence to: yagi@eng.niigata-u.ac.jp and znzahran@eng.niigata-u.ac.jp

Contents

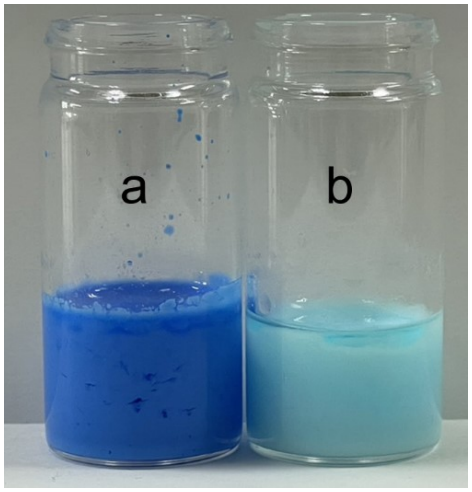

Figure S1. Photos of precursor suspensions containing $Cu(NO_3)_2$ and $Bi(NO_3)_3$ (a) with and (b) without MeIm.

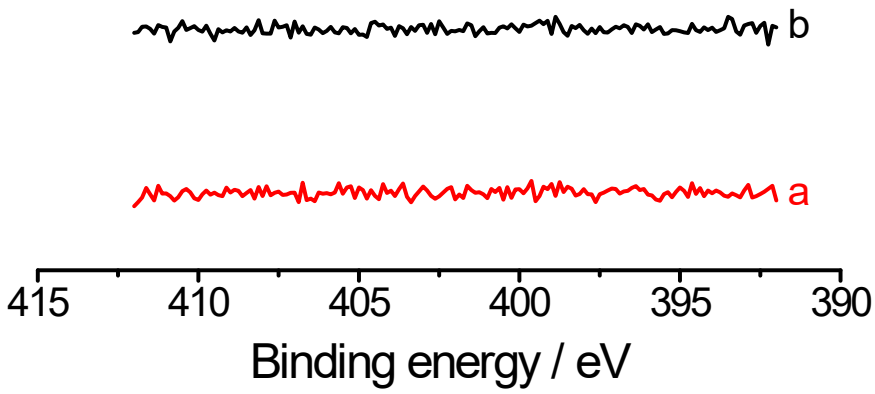

Figure S2. XPS spectra of (a) $CuBi_2O_4$(*w*) and (b) $CuBi_2O_4$(*w/o*) films in a N 1s region.

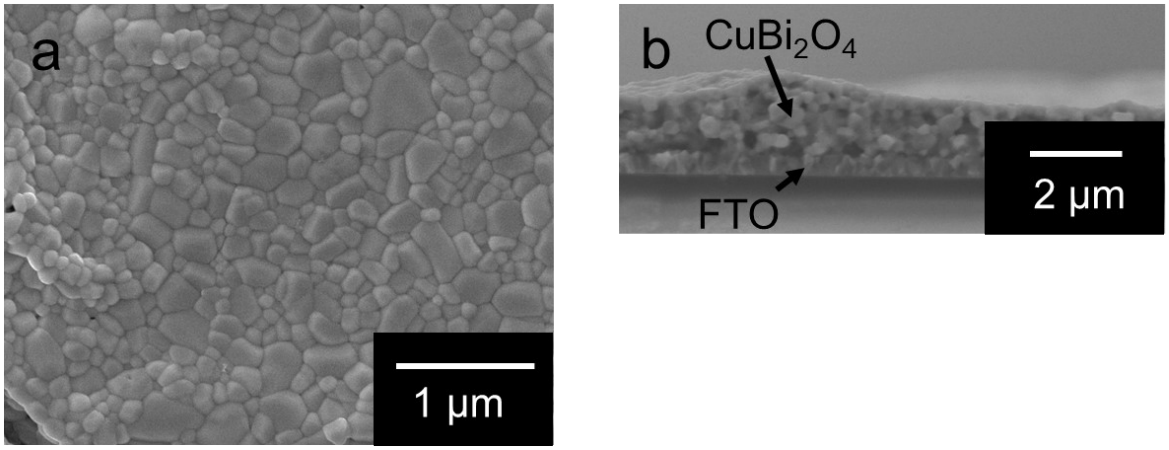

Figure S3. Top view SEM images (a) and cross-section view SEM images (b) of $CuBi_2O_4$(*w*) after CA at 0.41 V vs. RHE under O_2 for 1 hour.

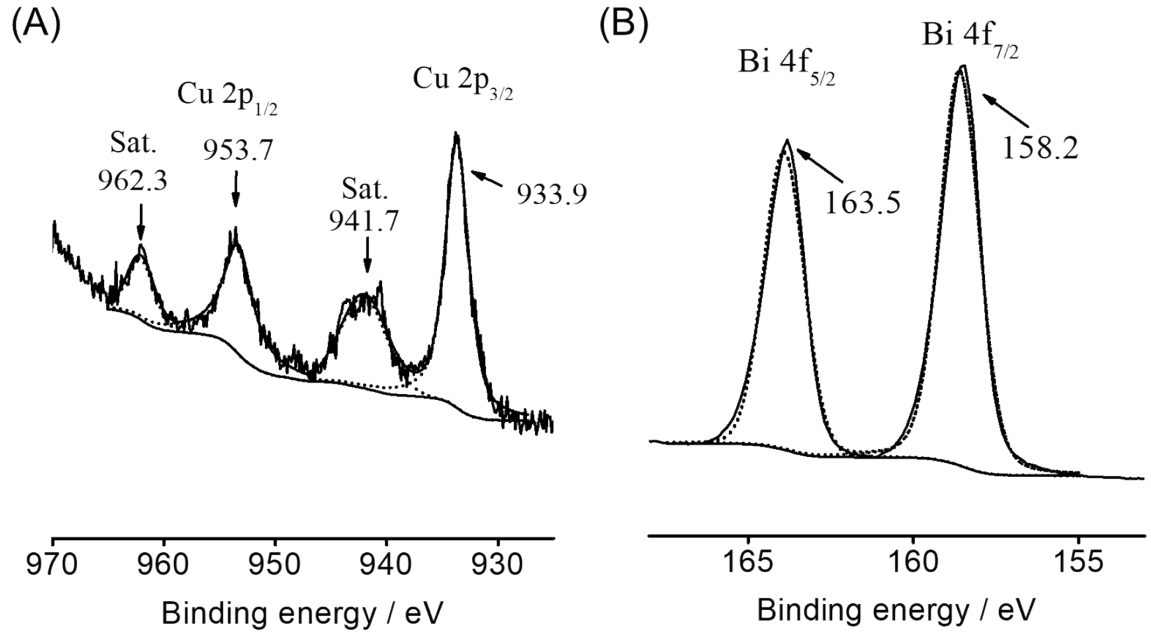

Figure S4. XPS spectra of $CuBi_2O_4$(*w*) after CA at 0.41 V vs. RHE under O_2 for 1 hour in (A) Cu 2*p* and (B) Bi 4*f* regions. The dotted lines show the deconvoluted bands.

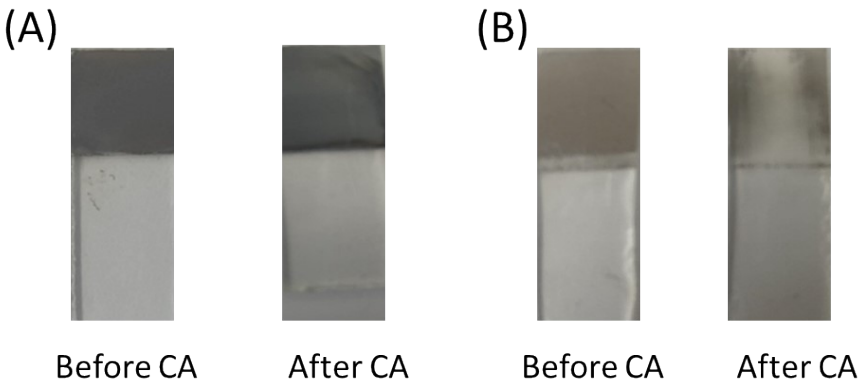

Figure S5. Photos of (A) $CuBi_2O_4$(*w*) and (B) $CuBi_2O_4$(*w/o*) films before (left) and after (right) CA at 0.41 V vs RHE under O_2 for 24 h.

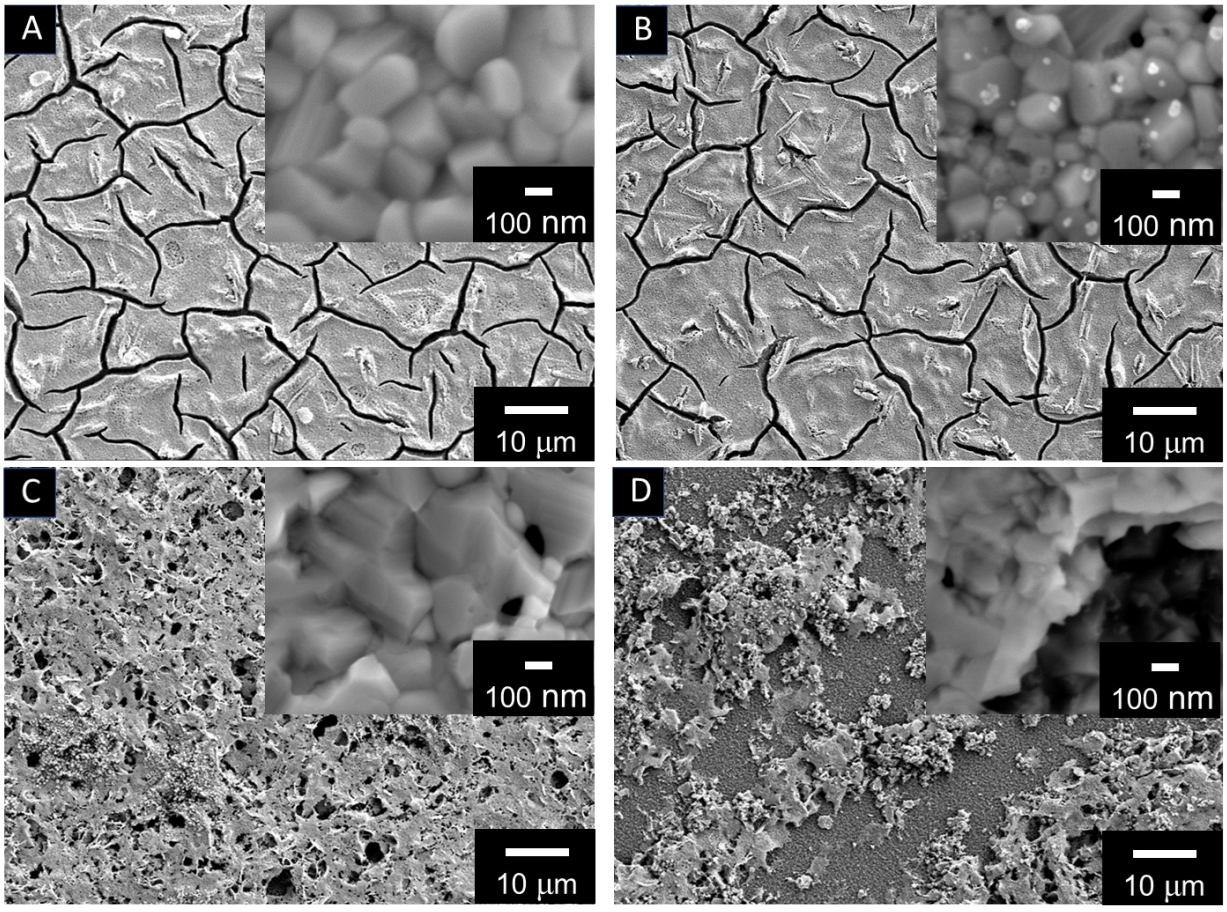

Figure S6. Top view SEM images of $CuBi_2O_4$(*w*) (A, B) and $CuBi_2O_4$(*w/o*) (C, D) films before (A, C) and after (B, D) CA at 0.41 V vs RHE under O_2 for 24 h.

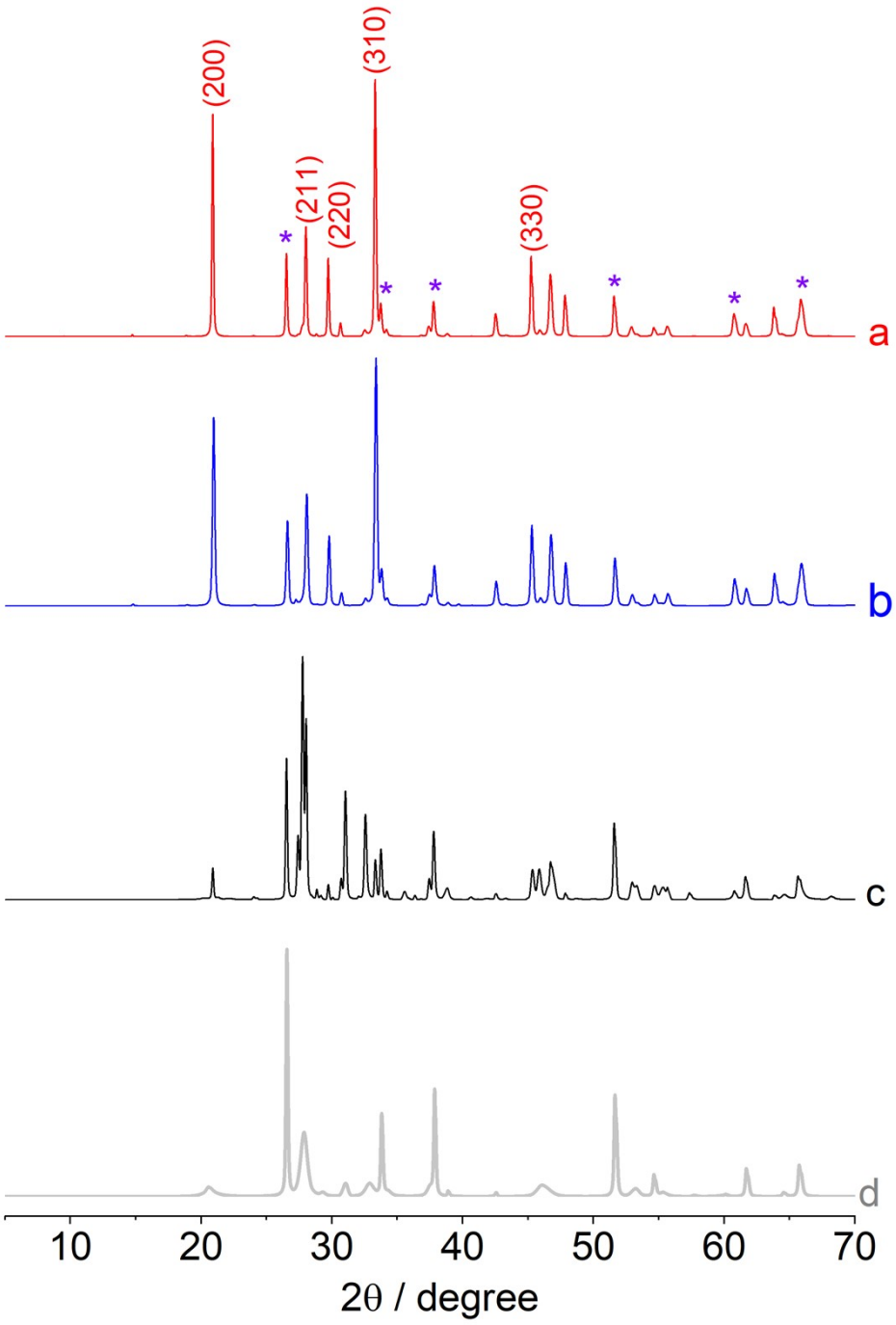

Figure S7. XRD patterns of $CuBi_2O_4$(*w*) (a, b) and $CuBi_2O_4$(*w/o*) (c, d) films before (a, c) and after (b, d) CA at 0.41 V vs RHE under O_2 for 24 h. The peaks of the FTO substrate are indicated by the purple asterisks in the spectrum a.

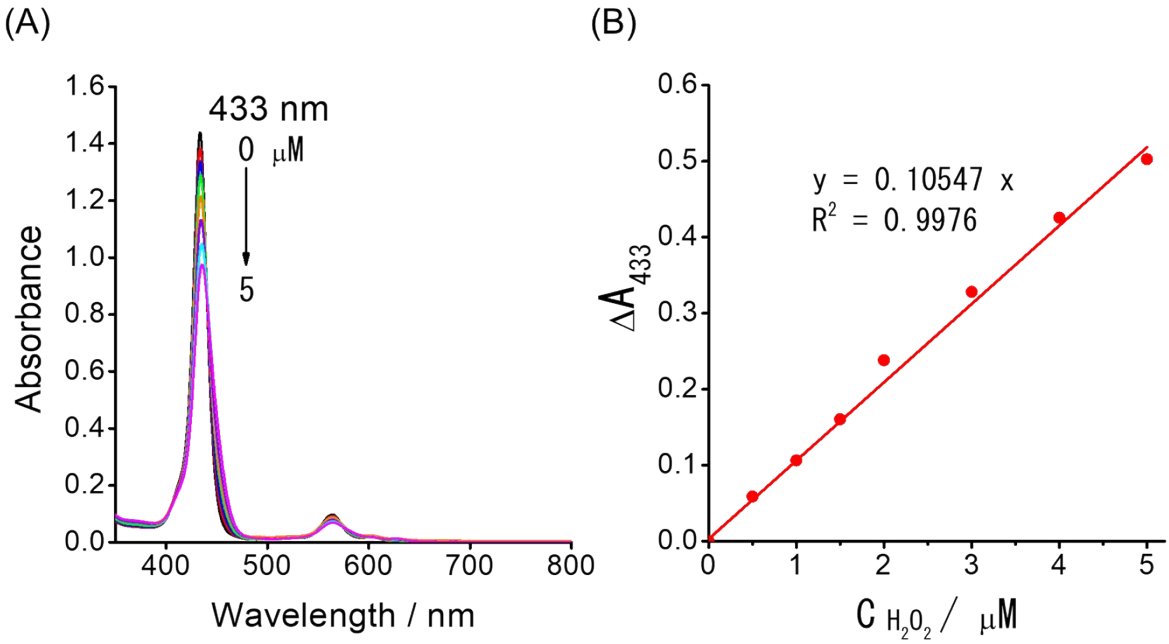

Figure S8. Calibration curve of hydrogen peroxide. (A) UV-visible absorption spectra of the aqueous solution (2.5 mL) containing 5 μM Ti-TPyP reagent, 5 mM HCl and 0.48 M HNO_3 with the various concentrations (c_{H2O2}) of hydrogen peroxide. (B) Relationship between the absorbance decrease (ΔA_{433}) at 433 nm and c_{H2O2}.

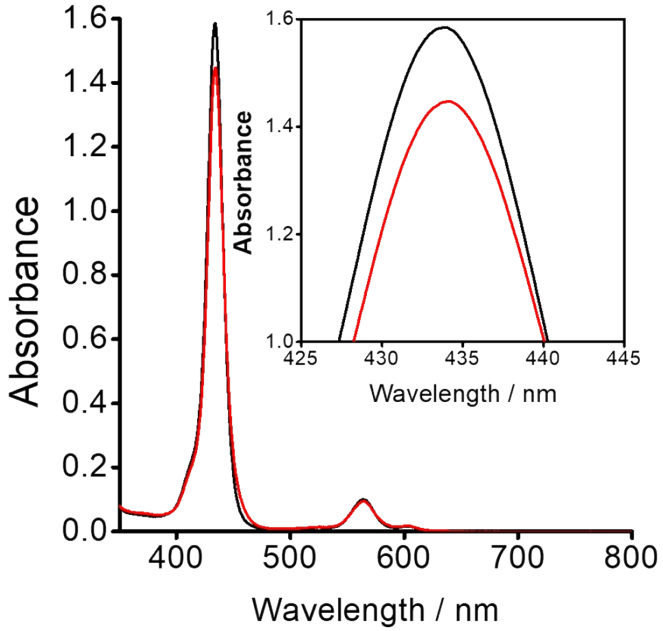

Figure S9. UV-visible absorption spectra of the aqueous solution (2.5 mL) containing 5 μM Ti-TPyP reagent, 5 mM HCl and 0.48 M HNO_3 with adding the electrolyte solutions before (black) and after (red) the bulk photoelectrolysis for ORR at 0.41 V vs. RHE under O_2 for 1 hour.

Table S1. Comparison of IPCE values among state-of-the-art $CuBi_2O_4$ photocathodes but being not exclusively for ORR.

Photocathodes	Preparation method	Conditions	Applied potential (V vs. RHE)	λ (nm)	IPCE (%)	Ref.
FTO/$CuBi_2O_4$(*w*)	MiMIC	0.1 M phosphate buffer solution (pH = 7.0) saturated with O_2	0.41	440	21	This work
FTO/$CuBi_2O_4$	Drop cast	0.3 M K_2SO_4 and 0.2 M phosphate buffer (pH 6.65) with H_2O_2	0.6	440	20	S1
FTO/$CuBi_2O_4$	Electrodeposition	0.1 M NaOH solution (pH 12.8) saturated with O_2	0.6	440	5	S2
FTO/$CuBi_2O_4$/Au/N,Cu−C [a)]	Thermal oxidation	0.3 M K_2SO_4/0.2 M phosphate buffer solution (pH 6.68) under Ar	0.65	440	3	S3
FTO/$CuBi_2O_4$	Spin coating	0.3 M K_2SO_4 and 0.2 M phosphate buffer (pH 6.65) with H_2O_2	0	440	27	S4
FTO/$CuBi_2O_4$/APTES [b)]	Electrodeposition and spin coating	0.1 M $KHCO_3$ solution (pH = 6.8) saturated with CO_2	0.4	440	4	S5
FTO/$CuBi_2O_4$	Electrodeposition	0.1M Na_2SO_4 (pH = 10.8) under Ar	0.2	440	0.5	S6
FTO/$CuBi_2O_4$	Spin coating	0.3 M K_2SO_4 and 0.2 M phosphate buffer (pH 6.65) with H_2O_2	0.6	440	30	S7

[a)] N, Cu-C : nitrogen/copper co-doped carbon nanosheet, [b)] APTES: 3-aminopropyltriethoxysilane.

References

S1 S. P. Berglund, F. F. Abdi, P. Bogdanoff, A. Chemseddine, D. Friedrich and R. Van De Krol, *Chem. Mater.*, 2016, **28**, 4231–4242.

S2 D. Kang, J. C. Hill, Y. Park and K. Choi, *Chem. Mater.*, 2016, **28**, 4331–4340.

S3 N. Xu, F. Li, L. Gao, H. Hu, Y. Hu, X. Long, J. Ma and J. Jin, *ACS Sustain. Chem. Eng.*, 2018, **6**, 7257–7264.

S4 D. A. Reddy, Y. Kim, P. Varma, M. Gopannagari, K. A. J. Reddy, D. H. Hong, I. Song, D. P. Kumar and T. K. Kim, *ACS Appl. Energy Mater.*, 2022, **5**, 6050–6058.
S5 J. Jin, J. Hu, J. Qu, G. Cao, Y. Lei, Z. Zheng, X. Yang and C. M. Li, *ACS Appl. Mater. Interfaces*, 2022, **14**, 17509–17519.
S6 N. T. Hahn, V. C. Holmberg, B. A. Korgel and C. B. Mullins, *J. Phys. Chem. C*, 2012, **116**, 6459–6466.
S7 Y. Xu, J. Jian, F. Li, W. Liu, L. Jia and H. Wang, *J. Mater. Chem. A*, 2019, **7**, 21997–22004.